JOURNAL OF GUIDANCE, CONTROL, AND DYNAMICS
Vol. 27, No. 2, March–April 2004

Boost-Phase Identification of Theater Ballistic Missiles Using Radar Measurements

Meirav Almogi-Nadler,* Yaakov Oshman,† and Joseph Z. Ben-Asher‡
Technion—Israel Institute of Technology, 32000 Haifa, Israel

This paper addresses the problem of identification of theater ballistic missiles during boost phase using radar measurements. Based on the use of the Wald sequential probability ratio test (SPRT), three identification algorithms are presented, corresponding to scenarios of increasing uncertainty. The use of the SPRT allows meeting specified false-alarm and missed-detection probabilities, while minimizing identification time. When the missiles' dynamic models and launch initial conditions (location and time) are completely and accurately known, the SPRT works directly with the raw radar measurements. In other scenarios, including a case where the launch location and launch time are unknown, two extended Kalman filters are used to generate the innovations sequences driving the SPRT. An extensive Monte Carlo simulation study is used to demonstrate the performance of the proposed procedures. Although the identification times and actual error probabilities depend, to some degree, on proper filter tuning, it is shown that reasonable mean identification times can be attained, corresponding to acceptable false-alarm and missed-detection rates, even in the presence of model uncertainties. This performance renders the proposed algorithms viable for the difficult problem considered.

I. Introduction

IT is widely recognized these days that theater ballistic missiles (TBM) impose a severe threat, which needs to be fully addressed on various levels. This paper is concerned with the operational level, where several ballistic-missile-defense (BMD) systems, belonging to competing concepts, have been proposed over the last decade. Some of these systems, such as the PAC-3 and the Arrow, have already demonstrated their ability to intercept nonmaneuvering TBMs with a hit-to-kill accuracy in controlled experiments[1,2] and have been declared operational.

Currently known TBMs are not designed to maneuver. Nevertheless, they have an inherent high maneuvering potential in the atmosphere, resulting from their very high reentry speed. The successful development of BMD systems, such as the PAC-3 and the Arrow, is expected to motivate the development of a new generation of maneuvering TBMs in the foreseeable future. Although a TBM is blind with respect to the interceptor, it can execute hard maneuvers randomly in order to avoid interception on its way to a designated surface target, while complying with the constraint of hitting it. A defense system that cannot guarantee that the miss distance generated by a target evasive maneuver will be sufficiently small will render the probability of an unacceptable leakage nonzero.

The TBM's trajectory can be divided into three phases: boost phase, midcourse, and the terminal phase. During the boost phase, the engine is operating and so is the guidance system. In the midcourse phase, which occurs mainly in space, the trajectory is essentially ballistic. In the terminal phase the ballistic missile reenters the atmosphere. It can be argued that the interception of a ballistic missile during its boost phase is superior to its interception in subsequent phases (which has been the underlying principle of BMD systems such as PAC-3 and Arrow). This is so because during the boost phase the ballistic missile is a huge, distinct, and especially vulnerable target, in contrast with the following phases during which hitting the target 1) is very difficult (and, hence, has been termed "shooting a bullet with a bullet" in the missile community) and 2) might not be sufficient for guaranteeing the required defense. During the midcourse phase, the missile's engine is off; hence, the TBM is more difficult to detect. In addition, the missile is in space, and the warhead can easily break up into many parts, including munitions and debris, which are hard to hit. The missile's dynamic behavior during boost phase is quite predictable and essentially nonmaneuvering. On the other hand, when the ballistic missile reenters the atmosphere it is extremely fast, maneuverable, and, consequently, very hard to intercept.[3] Moreover, as was demonstrated during the 1991 Gulf War, some ballistic missiles are not structurally well designed; hence, they tend to break up during their reentry and become unstable, rendering them difficult to intercept. Finally, boost-phase intercept (BPI) has the distinct strategic advantage of inducing a threat to the enemy because of the risk of explosion above enemy territory.

A feasible BPI defense system can be based on aerial platforms—manned aircraft or unmanned vehicles—equipped with search-and-track systems and armed with air-to-air missiles. The aerial platforms loiter above the enemy territory, detect the TBM, and launch the intercepting missiles to hit or divert the threat.[4] One of the most difficult challenges facing such a defense system is the fact that the boost-phase duration is relatively very short. The purpose of the search-and-track system of the platform is to identify the launched TBM within a short time interval, which lasts from the time the TBM is detected until a reasonable time prior to the end of the boost phase. This information, along with the target data and its current and future positions, is transmitted to the interceptor, enabling it to plan the required interception.

This paper is concerned with the problem of identifying the type of the TBM within the boost phase. Such a capability in this early stage of the flight is essential for planning the interceptor's trajectory and for determining the performance envelope of the entire system. The earlier is the TBM identification, the higher is the BPI success probability. Moreover, an early identification capability enables the reduction of the required interceptor velocity and maneuverability, or, alternatively, the enlargement of the platform's deployment area. In addition, such a system can operate as a warning system for the defended assets. The identification methods presented herein are based on Wald's sequential probability ratio test (SPRT).[5] Characterized by its ability to reach a decision between two hypotheses

Presented as Paper 2002-3893 at the AIAA Guidance, Navigation, Control Conference, Monterey, CA, 5–8 August 2002; received 31 October 2002; revision received 3 August 2003; accepted for publication 6 October 2003.

*Graduate Student, Department of Aerospace Engineering; meiravan@rafael.co.il.

†Associate Professor, Department of Aerospace Engineering; yaakov.oshman@technion.ac.il. Associate Fellow AIAA.

‡Associate Professor, Department of Aerospace Engineering; yossi@aerodyne.technion.ac.il.

using a minimal set of measurements while satisfying prespecified error probability constraints, the SPRT facilitates the identification of the launched TBM in minimal time, which, in turn, is essential for the success of the BPI system.

The boost-phase missile identification problem, dealt with here, can be viewed as a member of the broad class of problems of identification and classification of objects. For obvious reasons, this class of problems is of paramount importance in many applications. Automatic-target-recognition (ATR) systems aim at solving such problems via fusing information from an array of sensors, including electro-optical, infrared, radar, and other sensors. ATR systems deal with the identification of targets in the presence of clutter and with their classification, as well as with making the distinction between similar types of targets. A review of ATR systems is presented in Ref. 6. Bhanu[7] discusses the application of neural networks technology to ATR problems. The optimum character of the SPRT has rendered it a useful tool for ATR systems, and Jouny and Garber[8] present extensions of the SPRT to cases where the ATR system has to distinguish between more than two targets (simple hypotheses).

The remainder of this paper is organized as follows. In the next section the mathematical model of the TBM identification problem is defined. Three identification algorithms are then presented, corresponding to three different scenarios ordered according to increasing uncertainty. Results of an extensive Monte Carlo simulation study are then presented, which demonstrate the capability of the proposed algorithms. Concluding remarks are offered in the last section.

II. Problem Formulation

This paper is concerned with a scenario where two TBMs are present in the theater. Denote these missiles by TBM-A and TBM-B. The BPI aerial platform is a single unmanned vehicle, carrying a radar system that measures the range and the two line-of-sight (LOS) angles to the target. A typical scenario geometry is shown in Fig. 1. The search-and-track system uses the radar measurements to drive an estimator and a statistical test in order to identify the type of the launched missile. This scenario can form a basis for more complicated scenarios, such as when more than two types of TBMs are suspected, when a number of launchers are active or when a number of defending platforms are flying.

A. Target Model

The TBM's state vector is defined as

$$\boldsymbol{x} \triangleq [x \quad y \quad z \quad V \quad \gamma \quad \chi \quad a_n]^T \tag{1}$$

where x, y, and z are the TBM horizontal, sideways, and vertical coordinates, respectively, in an inertial system fixed to the launch location, V is the velocity, γ is the flight-path angle, χ is the azimuth launch angle, and a_n is the normal acceleration.

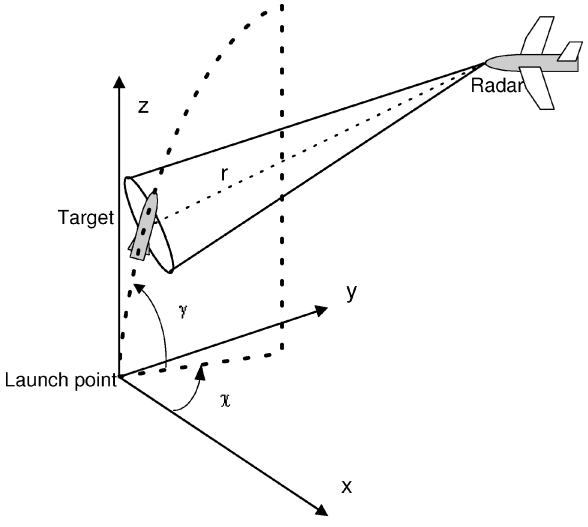

Fig. 1 TBM boost-phase interception geometry.

Typically, the duration of the estimation and identification process is very short (on the order of about 30 s). Hence, to simplify the ensuing analysis without losing generality it is assumed that the angle χ is constant throughout the estimation process and that the Earth is flat and nonrotating. In addition, it is assumed that the actual normal acceleration a_n obeys first-order dynamics with time constant τ, the TBM flies at zero sideslip angle, and the TBM's thrust is directed along the flight trajectory. The TBM equations of motion thus become

$$\dot{x} = V \cos\gamma \cos\chi \tag{2a}$$

$$\dot{y} = V \cos\gamma \sin\chi \tag{2b}$$

$$\dot{z} = V \sin\gamma \tag{2c}$$

$$\dot{V} = (T - D)/m - g \sin\gamma \tag{2d}$$

$$\dot{\gamma} = (-a_n - g \cos\gamma)/V \tag{2e}$$

$$\dot{\chi} = 0 \tag{2f}$$

$$\dot{a}_n = \left(a_n^C - a_n\right)\Big/\tau, \qquad a_n^C(t) \neq 0 \qquad \forall t \in [t_1, t_2] \tag{2g}$$

where a_n^C is the normal acceleration command, T and D are the engine thrust and aerodynamic drag, respectively, and g is the gravity acceleration. The normal acceleration command is active between t_1 and t_2 (measured from launch time) in order to achieve the required range with a predetermined cutoff time.

B. Measurement Model

Carried by the aerial platform, the radar system measures the slant range and the two LOS angles to the target. The measurement equation is

$$\boldsymbol{z}_k = \boldsymbol{h}_k(\boldsymbol{x}_k) + \boldsymbol{v}_k \tag{3}$$

The radar measurement vector is given by

$$\boldsymbol{h}_k(\boldsymbol{x}_k) = [\psi_k \quad \theta_k \quad r_k]^T$$

$$= \begin{bmatrix} \arctan\left(\dfrac{y_k - y_{r,k}}{x_k - x_{r,k}}\right) \\ \arcsin\left(\dfrac{z_k - z_{r,k}}{r_k}\right) \\ \sqrt{(x_{r,k} - x_k)^2 + (y_{r,k} - y_k)^2 + (z_{r,k} - z_k)^2} \end{bmatrix} \tag{4}$$

where ψ_k and θ_k are the azimuth and elevation LOS angles at time t_k, respectively, and r_k is the range to the TBM at time t_k. The vectors $[x_{r,k}, y_{r,k}, z_{r,k}]^T$ and $[x_k, y_k, z_k]^T$ denote the positions at time t_k of the aerial platform, which carries the radar system, and the TBM, respectively. Without loss of generality, it is assumed in this work that the radar's position is known and constant. This assumption is justified by noting that the duration of the decision process is very short and that the radar-carrying platform measures its own position with great accuracy (e.g., using an inertial navigation system and/or global positioning system).

The measurement noise $\boldsymbol{v}_k$ is modeled as a zero-mean, white, Gaussian sequence with known covariance, that is,

$$\boldsymbol{v}_k \sim \mathcal{N}(0, R_k) \tag{5}$$

where

$$R_k = \operatorname{diag}\left\{\sigma_\psi^2, \sigma_\theta^2, \sigma_r^2\right\} \tag{6}$$

III. Identification Algorithms

The TBM identification algorithms are based on the use of a statistical test for reaching a decision between the following null and alternate hypotheses, respectively:

$\mathcal{H}_0$: The observed TBM is TBM-A.

$\mathcal{H}_1$: The observed TBM is TBM-B.

To minimize the identification time, the statistical test used in this work is Wald's SPRT.[5,9] Devised in 1943 by Wald as the first solution of the general problem of sequential tests of statistical hypotheses, the SPRT is commonly applied in various fields such as failure detection and isolation,[10] radar target detection,[11,12] and automatic target recognition.[8] The SPRT considers the decision time as a random variable and aims at reaching a decision between the hypotheses in minimum time, while complying with the constraints of false-alarm and missed-detection probabilities as set by the designer. Conjectured by Wald in 1943, this optimum nature of the SPRT was proved in 1948 in a joint work with Wolfowitz.[13]

Remark 1: The problem addressed in this paper deals with the identification of two ballistic missiles. Nevertheless, complex cases dealing with more than two missiles can also be handled using similar principles. Thus, Ref. 8 treats the extension of the SPRT to more than two hypotheses in order to identify an aircraft target out of $M > 2$ possible targets, using radar measurements.

The SPRT is defined as follows. Observe the joint likelihood ratio, or equivalently the logarithm of the joint likelihood ratio Λ_n, defined as

$$\Lambda_n \equiv \Lambda(\mathcal{Z}^n) \triangleq \ell_n \frac{p\left(\mathcal{Z}^n \middle| \mathcal{H}_1\right)}{p\left(\mathcal{Z}^n \middle| \mathcal{H}_0\right)} \tag{7}$$

where $p(\mathcal{Z}^n|\mathcal{H}_i)$ is the the probability density function (PDF) of the measurements given the hypothesis $\mathcal{H}_i$, $i = 0, 1$.

A function of the observation sequence $\mathcal{Z}^n$, the log-likelihood ratio (LLR) Λ_n is calculated sequentially. The LLR value is then tested against two thresholds, $A > 0$ and $B < 0$, derived from the predetermined false-alarm and missed-detection probabilities α and β, respectively, according to

$$A = \ell_n[(1-\beta)/\alpha] \tag{8a}$$

$$B = \ell_n[\beta/(1-\alpha)] \tag{8b}$$

where α and β are defined by

$$\alpha = \text{Prob}\left(\mathcal{Z}^n \in \Gamma_1 \middle| \mathcal{H}_0\right) = \int_{\Gamma_1} p\left(\mathcal{Z}^n \middle| \mathcal{H}_0\right) \mathrm{d}Z \tag{9}$$

$$\beta = \text{Prob}\left(\mathcal{Z}^n \in \Gamma_0 \middle| \mathcal{H}_1\right) = \int_{\Gamma_0} p\left(\mathcal{Z}^n \middle| \mathcal{H}_1\right) \mathrm{d}Z \tag{10}$$

and Γ_0 and Γ_1 are the two disjoint subspaces, corresponding to the two hypotheses, composing the observation space Γ. The partition of the observation space Γ into Γ_0 and Γ_1 is such that the hypothesis $\mathcal{H}_0$ is accepted if the observations belong to Γ_0 and $\mathcal{H}_1$ is accepted if the observations are from Γ_1. The SPRT, which is designed to minimize the number of measurements required to make a decision while satisfying the specified error probabilities α and β, is defined as follows:

$$\text{Hypothesis accepted} = \begin{cases} \mathcal{H}_1 & \Lambda_n \geq A \\ \mathcal{H}_0 & \Lambda_n \leq B \\ \text{pending} & \text{otherwise} \end{cases} \tag{11}$$

When either of the thresholds is reached, a corresponding decision is made. Until such occurrence, the decision is postponed to the next observation sample.

Remark 2: Wald's SPRT assumes a static hypothesis structure, that is, one of the two given hypotheses is true and the other is false throughout the estimation process. A modified SPRT was proposed by Shiryayev,[14] in which a switch between the two hypotheses is allowed during the process. This property makes the modified SPRT suitable for fault detection and isolation applications,[15] where a certain component can function properly at the beginning of the process and then malfunction at a later stage (corresponding to a failure, which can be described as a switch from $\mathcal{H}_0$ to $\mathcal{H}_1$). In the case under consideration herein, the simpler Wald's SPRT is appropriate because no switch between the hypotheses (corresponding to the different missiles) is allowed.

The analysis presented in the sequel addresses three possible scenarios, corresponding to three levels of increasing uncertainty.

A. Complete Information

Assume that the launch location and launch time, as well as the launch azimuth angle and the TBM model, are accurately known. In most cases, this assumption would be unrealistic. Nevertheless, this case was analyzed in this work in order to provide a performance bound for the more realistic cases to be addressed in the sequel.

Because the radar measurement noise is white, the raw measurements in this case are statistically independent. Thus, the joint PDF of the measurement sequence given each hypothesis can be computed as the product of the marginal PDFs of all individual measurements in the sequence

$$p\left(\mathcal{Z}^n \middle| \mathcal{H}_i\right) = \prod_{k=1}^{n} p(\boldsymbol{z}_k|\mathcal{H}_i) \tag{12}$$

The LLR is given, in this case, by

$$\Lambda(\mathcal{Z}^n) \triangleq \ell_n \frac{p\left(\mathcal{Z}^n \middle| \mathcal{H}_1\right)}{p\left(\mathcal{Z}^n \middle| \mathcal{H}_0\right)} = \ell_n \prod_{k=1}^{n} \frac{p(\boldsymbol{z}_k|\mathcal{H}_1)}{p(\boldsymbol{z}_k|\mathcal{H}_0)} \tag{13}$$

Notice that the LLR is given here as a function of the sample size, which is a random variable. To calculate the LLR, the PDF of each measurement in the observation sequence needs to be calculated for each of the two hypotheses. To that end, notice that if TBM-A was launched (corresponding to the null hypothesis) the measurement equation is given by

$$\boldsymbol{z}_k = \boldsymbol{h}\left(\boldsymbol{x}_k^A\right) + \boldsymbol{v}_k, \qquad \boldsymbol{v}_k \sim \mathcal{N}(0, R_k) \tag{14}$$

where $\boldsymbol{x}_k^A$ is the state vector corresponding to TBM-A, that is, the measurement sequence in this case is white, Gaussian, with mean and covariance

$$\boldsymbol{z}_k|\mathcal{H}_0 \sim \mathcal{N}\left(\boldsymbol{h}\left(\boldsymbol{x}_k^A\right), R_k\right) \tag{15}$$

To formulate the measurement equation in case TBM-B was launched, assume that an additive, time-varying bias distinguishes between the two missiles' state vectors, that is,

$$\boldsymbol{x}_k^B = \boldsymbol{x}_k^A + \boldsymbol{b}_k \tag{16}$$

This facilitates writing the expression for the measurement corresponding to TBM-B as a function of TBM-A's state

$$\boldsymbol{h}\left(\boldsymbol{x}_k^B\right) = \boldsymbol{h}\left(\boldsymbol{x}_k^A + \boldsymbol{b}_k\right) \tag{17}$$

In practice, it is known that the differences between the trajectories of similar theater ballistic missiles (e.g., SCUD-B and SCUD-C) during the boost phase are minor, as shown in Fig. 2. Therefore, Eq. (17) can be approximated using a first-order Taylor expansion as

$$\boldsymbol{h}\left(\boldsymbol{x}_k^B\right) \approx \boldsymbol{h}\left(\boldsymbol{x}_k^A\right) + \left[\nabla_x \boldsymbol{h}^T\left(\boldsymbol{x}_k^A\right)\right]^T \boldsymbol{b}_k \tag{18}$$

where the matrix $\nabla_x \boldsymbol{h}^T$ denotes the gradient of the measurement vector. Thus, given a TBM-B launch (corresponding to the alternate hypothesis) the measurement equation is given by

$$\boldsymbol{z}_k \approx \boldsymbol{h}\left(\boldsymbol{x}_k^A\right) + \left[\nabla_x \boldsymbol{h}^T\left(\boldsymbol{x}_k^A\right)\right]^T \boldsymbol{b}_k + \boldsymbol{v}_k \tag{19}$$

yielding

$$\boldsymbol{z}_k|\mathcal{H}_1 \sim \mathcal{N}\left(\left\{\boldsymbol{h}\left(\boldsymbol{x}_k^A\right) + \left[\nabla_x \boldsymbol{h}^T\left(\boldsymbol{x}_k^A\right)\right]^T \boldsymbol{b}_k\right\}, R_k\right) \tag{20}$$

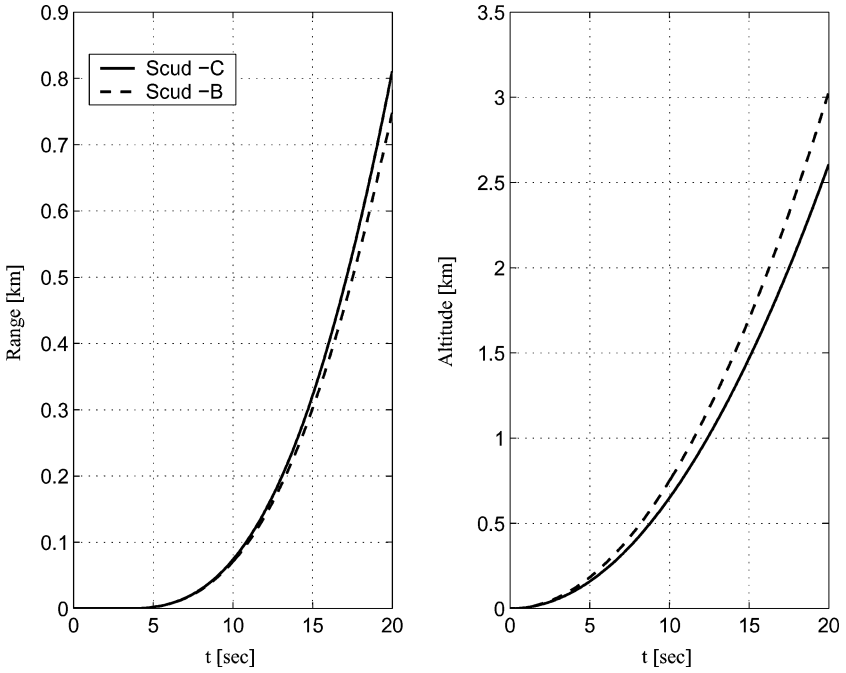

a) b)

Fig. 2 Boost-phase trajectories of SCUD-B and SCUD-C: a) horizontal component of slant range to missiles and b) vertical component of slant range to missiles.

The PDFs of the measurement samples given the two hypotheses are, thus, given by

$$p(z_k|\mathcal{H}_0) = \left(1/\sqrt{2\pi|R_k|}\right)\exp\left\{-\tfrac{1}{2}\left[z_k - \boldsymbol{h}\left(\boldsymbol{x}_k^A\right)\right]^T R_k^{-1}\left[z_k - \boldsymbol{h}\left(\boldsymbol{x}_k^A\right)\right]\right\} \quad (21)$$

and

$$p(z_k|\mathcal{H}_1) = \left(1/\sqrt{2\pi|R_k|}\right)\exp\left(-\tfrac{1}{2}\left\{z_k - \boldsymbol{h}\left(\boldsymbol{x}_k^A\right) - \left[\nabla_x \boldsymbol{h}^T\left(\boldsymbol{x}_k^A\right)\right]^T \boldsymbol{b}_k\right\}^T \times R_k^{-1}\left\{z_k - \boldsymbol{h}\left(\boldsymbol{x}_k^A\right) - \left[\nabla_x \boldsymbol{h}^T\left(\boldsymbol{x}_k^A\right)\right]^T \boldsymbol{b}_k\right\}\right) \quad (22)$$

The LLR for the kth measurement is given by

$$u_k = \ell_n \frac{p(z_k|\mathcal{H}_1)}{p(z_k|\mathcal{H}_0)} = \left\{z_k - \boldsymbol{h}\left(\boldsymbol{x}_k^A\right) - \frac{1}{2}\left[\nabla_x \boldsymbol{h}^T\left(\boldsymbol{x}_k^A\right)\right]^T \boldsymbol{b}_k\right\}^T \times R_k^{-1}\left[\nabla_x \boldsymbol{h}^T\left(\boldsymbol{x}_k^A\right)\right]^T \boldsymbol{b}_k \quad (23)$$

Thus the LLR for n statistically independent measurements is given by

$$\Lambda_n = \sum_{k=1}^{n}\left\{z_k - \boldsymbol{h}\left(\boldsymbol{x}_k^A\right) - \frac{1}{2}\left[\nabla_x \boldsymbol{h}^T\left(\boldsymbol{x}_k^A\right)\right]^T \boldsymbol{b}_k\right\}^T R_k^{-1}\left[\nabla_x \boldsymbol{h}^T\left(\boldsymbol{x}_k^A\right)\right]^T \boldsymbol{b}_k \quad (24)$$

B. Staring Radar

In this scenario the assumptions of known launch location and launch azimuth angle are relaxed. It is still assumed that the launch time is known. This is a typical case for a radar staring at the target area, which is capable of accurately observing the launch time without being able to pinpoint the specific location of the launch. Here the measurements are statistically dependent as a result of initial condition uncertainty, and, therefore,

$$p\left(\mathcal{Z}^n\middle|\mathcal{H}_i\right) \neq \prod_{k=1}^{n} p(z_k|\mathcal{H}_i) \quad (25)$$

To use the SPRT in this case, the joint PDF of the measurement history is written in terms of the conditional PDF product

$$p(\mathcal{Z}^n) = \prod_{k=1}^{n} p\left(z_k\middle|\mathcal{Z}^{k-1}\right) \quad (26)$$

where $p(z_1|\mathcal{Z}^0) = p(z_1)$. To compute the conditional PDF product on the right-hand side of Eq. (26), we use the innovations process defined as

$$\tilde{z}_{k|k-1} \triangleq z_k - \hat{z}_{k|k-1} \quad (27)$$

where the predicted measurement is

$$\hat{z}_{k|k-1} = E\left\{z_k\middle|\mathcal{Z}^{k-1}\right\} \quad (28)$$

Computed internally by the Kalman filter, the innovations process is zero mean, white, Gaussian distributed with

$$\tilde{z}_{k|k-1} \sim \mathcal{N}\left(0,\, H_k P_{k|k-1} H_k^T + R_k\right) \quad (29)$$

where H_k is the measurement matrix (the Jacobian of the nonlinear measurement function) and $P_{k|k-1}$ is the covariance matrix of the prediction error. The conditional PDF of the kth measurement sample given all previous measurements is given by

$$p\left(z_k\middle|\mathcal{Z}^{k-1}\right) = 1\Big/\left[(2\pi)^{N/2}\left|\mathrm{cov}\left\{z_k\middle|\mathcal{Z}^{k-1}\right\}\right|^{\frac{1}{2}}\right] \times \exp\left\{-\tfrac{1}{2}\left[z_k - E\left\{z_k\middle|\mathcal{Z}^{k-1}\right\}\right]^T \mathrm{cov}\left\{z_k\middle|\mathcal{Z}^{k-1}\right\}^{-1} \times \left[z_k - E\left\{z_k\middle|\mathcal{Z}^{k-1}\right\}\right]\right\} \quad (30)$$

Using Eqs. (27) and (28) in Eq. (30) yields

$$p\left(z_k\middle|\mathcal{Z}^{k-1}\right) = 1\Big/\left[(2\pi)^{N/2}\left|\mathrm{cov}\left\{z_k\middle|\mathcal{Z}^{k-1}\right\}\right|^{\frac{1}{2}}\right] \times \exp\left\{-\tfrac{1}{2}\tilde{z}_{k|k-1}^T \mathrm{cov}\left\{z_k\middle|\mathcal{Z}^{k-1}\right\}^{-1}\tilde{z}_{k|k-1}\right\} \quad (31)$$

where $\mathrm{cov}\{z_k|\mathcal{Z}^{k-1}\}$ is the covariance of the innovations process

$$\mathrm{cov}\left\{z_k\middle|\mathcal{Z}^{k-1}\right\} = \mathrm{cov}\{\tilde{z}_{k|k-1}\} \quad (32)$$

Therefore, the conditional PDF of the measurement can be computed via the PDF of the innovations process

$$p\left(\boldsymbol{z}_k \middle| \mathcal{Z}^{k-1}\right) = p(\tilde{\boldsymbol{z}}_{k|k-1}) \tag{33}$$

which expresses the known fact that the measurement and innovations processes are causally invertible.[16] Because the innovations process is Gaussian and white,

$$p(\mathcal{Z}^n) = \prod_{k=1}^{n} p\left(\boldsymbol{z}_k \middle| \mathcal{Z}^{k-1}\right) = \prod_{k=1}^{n} p(\tilde{\boldsymbol{z}}_{k|k-1}) \tag{34}$$

Using the last result, the LLR can be computed as

$$\Lambda(\mathcal{Z}^n) = \ell_n \frac{p\left(\mathcal{Z}^n \middle| \mathcal{H}_1\right)}{p\left(\mathcal{Z}^n \middle| \mathcal{H}_0\right)} = \ell_n \frac{\prod_{k=1}^{n} p(\tilde{\boldsymbol{z}}_{k|k-1}|\mathcal{H}_1)}{\prod_{k=1}^{n} p(\tilde{\boldsymbol{z}}_{k|k-1}|\mathcal{H}_0)} \tag{35}$$

To compute the PDFs of the innovations appearing in Eq. (35), two extended Kalman filters (EKFs) are used, corresponding to the two hypotheses. Denote the EKF corresponding to the null hypothesis (TBM-A) by EKF-0 and the EKF corresponding to the alternate hypothesis (TBM-B) by EKF-1. The EKFs utilize the TBM differential equations (2), where the acceleration profiles are derived by propagating Eq. (2g) for nominal values of the acceleration commands and time constants.

Define the state vector of both EKFs as

$$\boldsymbol{x}_{\text{st}} = [x \quad y \quad z \quad V \quad \gamma \quad \chi]^T \tag{36}$$

The state variables satisfy the following differential equations:

$$\dot{x} = V\cos\gamma\cos\chi + w_x \tag{37a}$$

$$\dot{y} = V\cos\gamma\sin\chi + w_y \tag{37b}$$

$$\dot{z} = V\sin\gamma + w_z \tag{37c}$$

$$\dot{V} = (T - D)/m - g\sin\gamma + w_v \tag{37d}$$

$$\dot{\gamma} = (-a_n - g\cos\gamma)/V + w_\gamma \tag{37e}$$

$$\dot{\chi} = w_\chi \tag{37f}$$

where $\boldsymbol{w}_{\text{st}} = [w_x, w_y, w_z, w_v, w_\gamma, w_\chi]^T$ is a white, Gaussian noise process with

$$E\left\{\boldsymbol{w}_{\text{st}}(t)\boldsymbol{w}_{\text{st}}^T(s)\right\} = Q_{\text{st}}(t)\delta(t-s) \tag{38}$$

and

$$Q_{\text{st}} = \text{diag}\{q_x, q_y, q_z, q_v, q_\gamma, q_\chi\} \tag{39}$$

The noise intensity matrix $Q_{\text{st}}(t)$ is used to tune the EKF in cases where model parameter uncertainty is considered. It is assumed that the initial state is Gaussian distributed with

$$\boldsymbol{x}_{\text{st}}(0) \sim \mathcal{N}(\boldsymbol{\mu}_{\text{st}}(0), P_{\text{st}}(0)) \tag{40}$$

where

$$\mu_{\text{st}}(0) = [\mu_x(0) \quad \mu_y(0) \quad \mu_z(0) \quad \mu_v(0) \quad \mu_\gamma(0) \quad \mu_\chi(0)]^T \tag{41a}$$

$$P_{\text{st}}(0) = \text{diag}\{P_x(0), P_y(0), P_z(0), P_v(0), P_\gamma(0), P_\chi(0)\} \tag{41b}$$

The LLR for the kth measurement sample is given by

$$\begin{aligned} u_k = {} & \tfrac{1}{2}\ell_n\left|H_k^0 P_{k|k-1}^0 \left(H_k^0\right)^T + R_k\right| - \tfrac{1}{2}\ell_n\left|H_k^1 P_{k|k-1}^1 \left(H_k^1\right)^T + R_k\right| \\ & - \tfrac{1}{2}\left(\tilde{\boldsymbol{z}}_{k|k-1}^T \middle| \mathcal{H}_1\right)\left[H_k^1 P_{k|k-1}^1 \left(H_k^1\right)^T + R_k\right]^{-1}\left(\tilde{\boldsymbol{z}}_{k|k-1}^T \middle| \mathcal{H}_1\right) \\ & + \tfrac{1}{2}\left(\tilde{\boldsymbol{z}}_{k|k-1}^T \middle| \mathcal{H}_0\right)\left[H_k^0 P_{k|k-1}^0 \left(H_k^0\right)^T + R_k\right]^{-1}\left(\tilde{\boldsymbol{z}}_{k|k-1}^T \middle| \mathcal{H}_0\right) \end{aligned} \tag{42}$$

where the indices 0 and 1 indicate that the associated variables are computed using EKF-0 and EKF-1, respectively. The SPRT is implemented by testing the LLR

$$\Lambda(\mathcal{Z}^n) = \sum_{k=1}^{n} u_k \tag{43}$$

against the two thresholds computed previously, as detailed in Eq. (11).

C. Search Radar

In this scenario a search radar is considered, which acquires the target without having specific knowledge about its launch location and launch time. Thus, in addition to other variables already

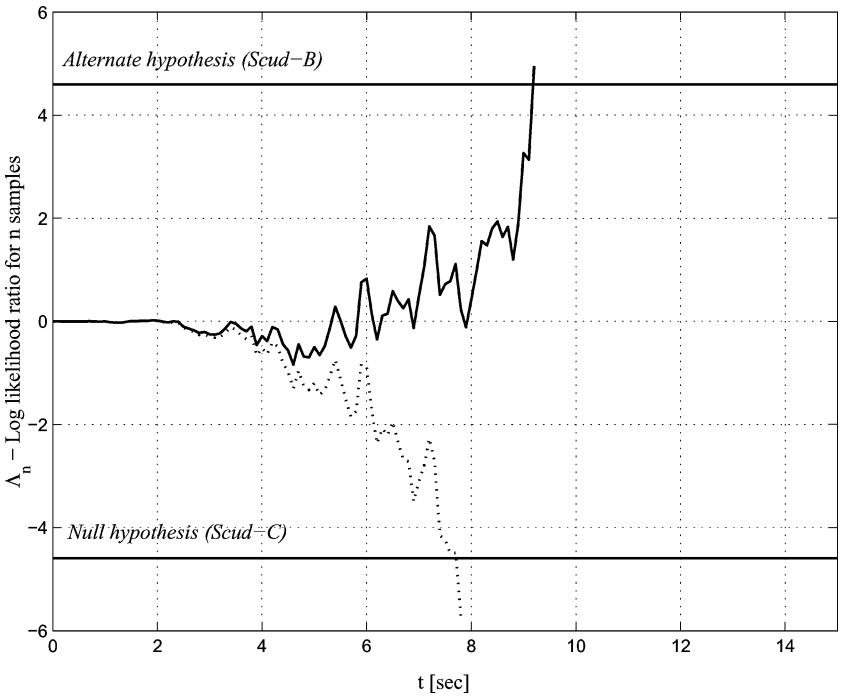

Fig. 3 Typical behavior of the SPRT—complete information: . . . ., SCUD-C launched and ——, SCUD-B launched.

estimated, in this case the launch time needs to be estimated as well. To this end, the launch time needs to be explicitly introduced into the mathematical model. This is done by first calculating the nominal flight-path angle for each TBM using Eqs. (2e) and (2g). Then, the differential equation of the flight-path angle [Eq. (2e)] is replaced by a polynomial expressing the flight-path angle as a function of two time variables: 1) t_0, the duration from the unknown launch time until the target acquisition by the radar, and 2) t, the running time from acquisition to identification.

Define the state vector of both EKFs in this case as

$$\boldsymbol{x}_{\mathrm{sr}} = [x \quad y \quad z \quad V \quad \chi \quad t_0]^T \tag{44}$$

The state variables satisfy the following differential equations:

$$\dot{x} = V\cos\gamma(t_0,t)\cos\chi + w_x \tag{45a}$$

$$\dot{y} = V\cos\gamma(t_0,t)\sin\chi + w_y \tag{45b}$$

$$\dot{z} = V\sin\gamma(t_0,t) + w_z \tag{45c}$$

$$\dot{V} = (T-D)/m(t_0,t) - g\sin\gamma(t_0,t) + w_v \tag{45d}$$

$$\dot{\chi} = w_\chi \tag{45e}$$

$$\dot{t}_0 = w_{t_0} \tag{45f}$$

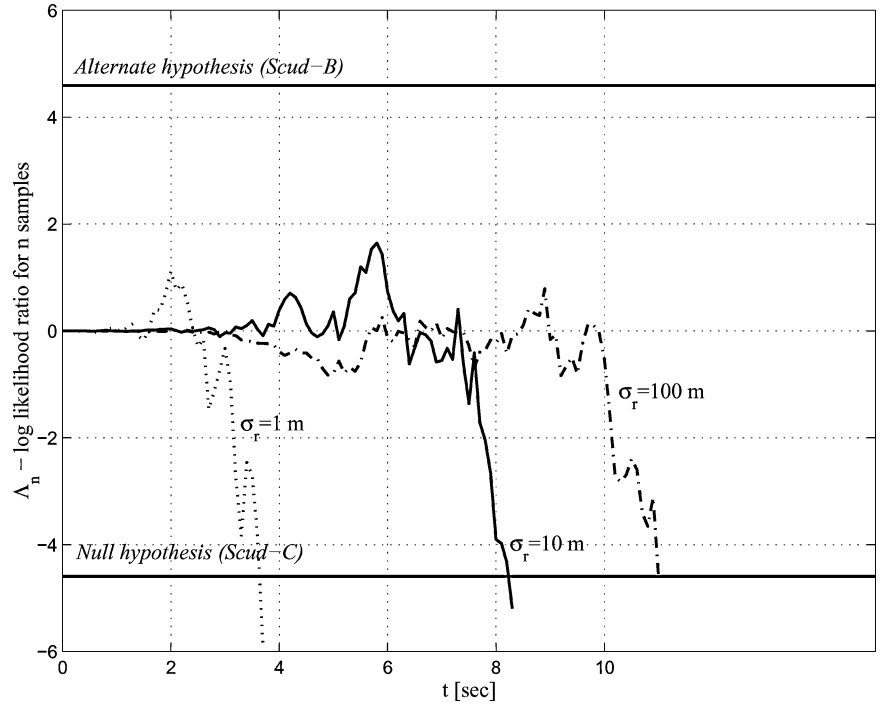

a)

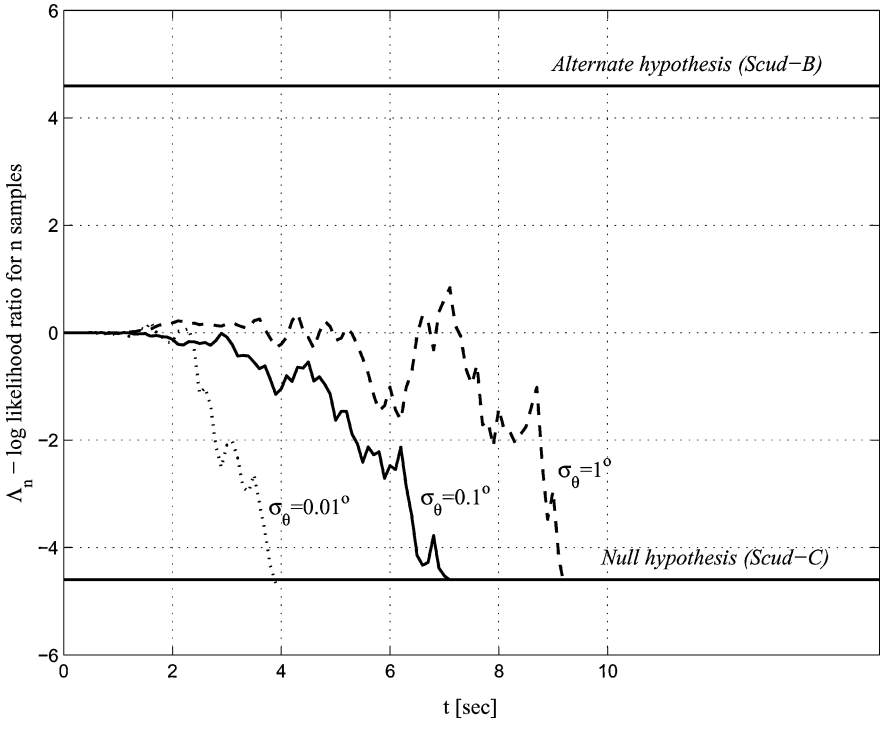

b)

Fig. 4 SPRT operation as a function of measurement noise standard deviation: a) range and b) elevation.

where $\boldsymbol{w}_{\rm sr} = [w_x, w_y, w_z, w_v, w_\chi, w_{t_0}]^T$ is a white, Gaussian noise process with

$$E\left\{\boldsymbol{w}_{\rm sr}(t)\boldsymbol{w}_{\rm sr}^T(s)\right\} = Q_{\rm sr}(t)\delta(t-s) \tag{46}$$

and

$$Q_{\rm sr} = \text{diag}\left\{q_x, q_y, q_z, q_v, q_\chi, q_{t_0}\right\} \tag{47}$$

The noise intensity matrix $Q_{\rm sr}(t)$ is used to tune the EKF in cases where model parameter uncertainty is considered. It is assumed that the initial state is Gaussian distributed with

$$\boldsymbol{x}_{\rm sr}(0) \sim \mathcal{N}(\boldsymbol{\mu}_{\rm sr}(0), P_{\rm sr}(0)) \tag{48}$$

where

$$\mu_{\rm sr}(0) = \left[\mu_x(0) \quad \mu_y(0) \quad \mu_z(0) \quad \mu_v(0) \quad \mu_\chi(0) \quad \mu_{t_0}(0)\right]^T \tag{49a}$$

$$P_{\rm sr}(0) = \text{diag}\left\{P_x(0), P_y(0), P_z(0), P_v(0), P_\chi(0), P_{t_0}(0)\right\} \tag{49b}$$

The TBM's flight-path angle and mass variation with time are given by the following polynomials:

$$\gamma(t_0,t) = \begin{cases} \pi/2 & 0 \le t_0+t \le t_1 \\ a_1(t_0+t)^4 + a_2(t_0+t)^3 + a_3(t_0+t)^2 + a_4(t_0+t) + a_5 & t_1 < t_0+t \le t_3 \\ b_1(t_0+t)^4 + b_2(t_0+t)^3 + b_3(t_0+t)^2 + b_4(t_0+t) + b_5 & t_3 < t_0+t < t_4 \end{cases} \tag{50}$$

$$m(t_0,t) = \begin{cases} m - \dot{m}(t_0+t) & 0 < t_0+t \le t_{\rm co} \\ m - \dot{m}t_{\rm co} & t_0+t > t_{\rm co} \end{cases} \tag{51}$$

The flight-path angle's polynomial coefficients and the trajectory segment end times t_3 and t_4 were chosen to best fit (in a least-squares sense) the nominal curves. The engine cutoff time is $t_{\rm co}$. The TBM's mass m also varies as a function of t_0 and t.

IV. Simulation Study

A numerical simulation study was carried out in order to demonstrate the performance of the proposed TBM identification method. The TBMs assumed in this study are SCUD-C, corresponding to the null hypothesis $\mathcal{H}_0$, and SCUD-B, corresponding to the alternate hypothesis $\mathcal{H}_1$. The model parameters of both missiles were estimated based on data appearing in Ref. 17. These parameters are summarized in Table 1. In the scenario analyzed one TBM launcher is located at the origin of the reference frame (see Fig. 1). The radar coordinates in the reference frame are $[x_r, y_r, z_r] = [100, 10, 10]$ km.

Figure 2 shows the boost-phase trajectories of both missiles under consideration. As can be clearly observed, the boost trajectories of both missiles are very similar, which renders the identification problem rather difficult.

The measurements are sampled at a frequency of 10 Hz and are contaminated by an additive zero-mean Gaussian noise with standard deviations of

$$\sigma_\theta = \sigma_\psi = 1.75 \text{ mrad}, \qquad \sigma_r = 10 \text{ m} \tag{52}$$

The false-alarm and missed-detection probabilities are set to be

$$\alpha = \beta = 0.01 \tag{53}$$

with corresponding threshold values

$$A = 4.6, \qquad B = -4.6 \tag{54}$$

The three cases analyzed in the preceding section are considered in the sequel.

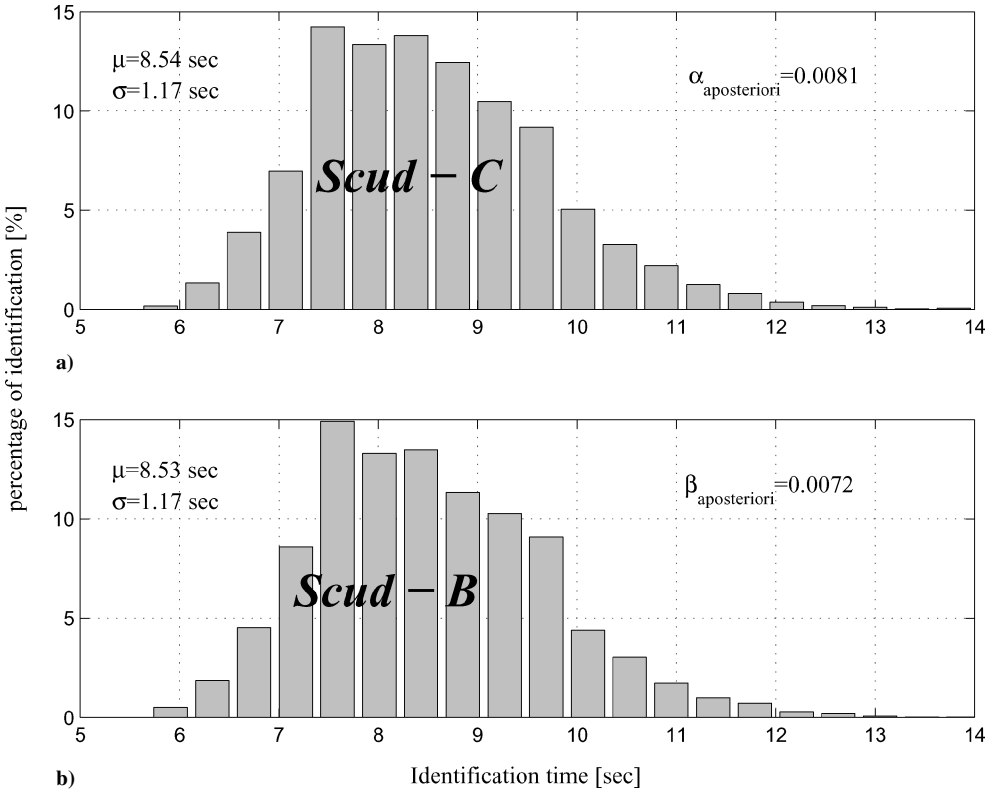

Fig. 5 Identification time histogram in a Monte-Carlo simulation. Complete information: a) SCUD-C launched and b) SCUD-B launched.

Table 1 TBM model parameters

Parameter	SCUD-B	SCUD-C
Range, km	300	500
m_0, kg	5900	6400
t_{co}, s	60	72
$\dot{m}$, kg/s	62.5	62.5
t_1, s	3	3
t_2, s	15	15
a_n^C, m/s^2	2	2
τ, s	1	1

A. Simulation Results

1. Complete Information

In this case the launch location and launch time are assumed known. Figure 3 demonstrates the performance of the SPRT for both TBMs in a typical case. It can be observed that a SCUD-C launch is identified at about 7.5 s, whereas a SCUD-B launch is identified at about 9 s.

Figure 4 shows the performance of the SPRT as a function of the measurement noise intensity. As could be expected, higher measurement noise results in delayed identification.

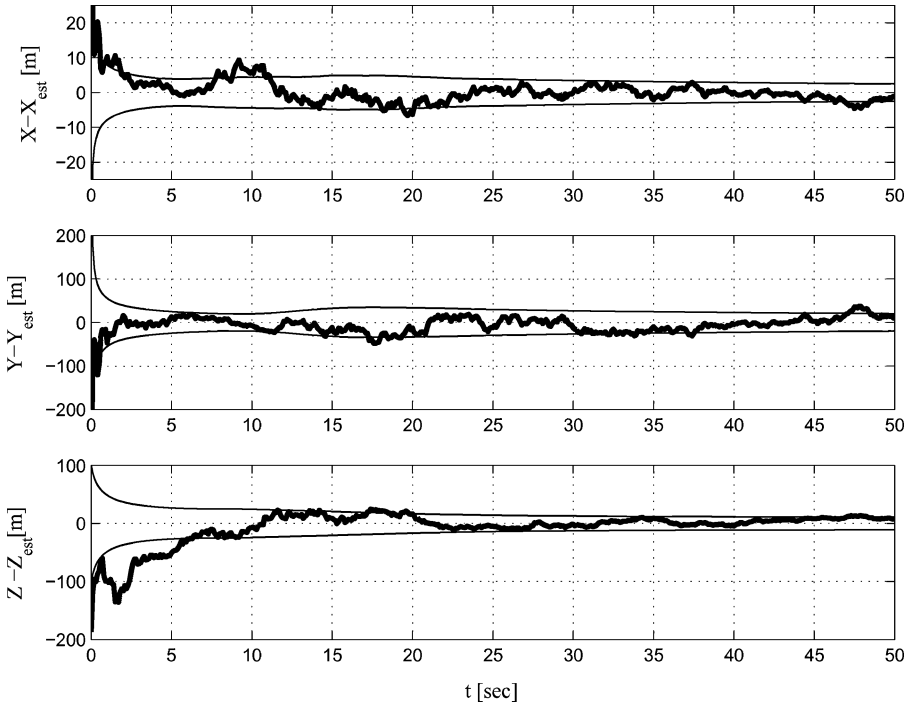

a) EKF-0

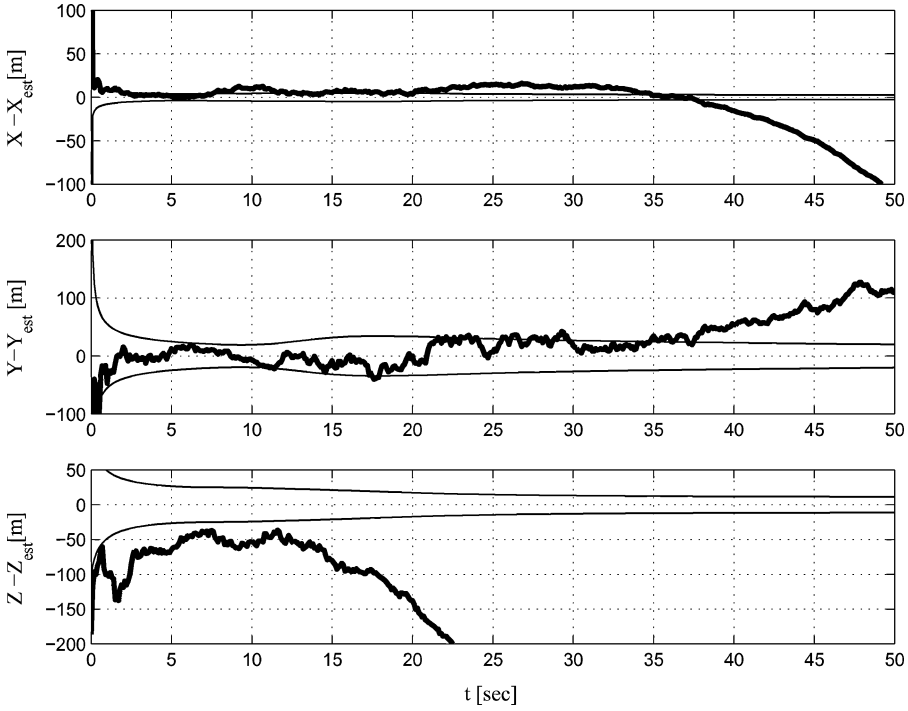

b) EKF-1

Fig. 6 Position estimation errors, SCUD-C launch, staring radar: ——, estimation error; ——, 1-σ envelope (as computed by filter).

Figure 5 presents a statistical analysis of the performance of the SPRT, as observed using Monte Carlo simulations with the measurement noise model of Eq. (52). The upper plot shows the identification time histogram corresponding to 10,000 SCUD-C launches (corresponding to the $\mathcal{H}_0$ hypothesis). The observed false-alarm rate is 0.0081, and the mean identification time is 8.54 s. The lower plot shows the corresponding result in the case of 10,000 SCUD-B launches (corresponding to the $\mathcal{H}_1$ hypothesis). In this case the observed missed-detection rate is 0.0072, and the mean identification time is 8.53 s. In both cases the observed error rates do not exceed the predetermined error probabilities.

As already mentioned, this unrealistic case of complete information serves to obtain bounds on the attainable performance of the proposed algorithms in more realistic cases. These cases are presented next.

2. Staring Radar

In this case the launch time is assumed known, while the launch location is assumed unknown. The statistical moments of the initial state vector are summarized in Tables 2 and 3. The process noise intensity used in this case is $Q_{\text{st}}(t) = 0$.

Figure 6 shows the TBM position estimation errors as generated by the two EKFs associated with the SPRT. In both cases the missile launched is SCUD-C. As evident from Fig. 6, EKF-0 (designed about the $\mathcal{H}_0$ hypothesis) performs well, contrary to EKF-1 (designed about the $\mathcal{H}_1$ hypothesis). These results correlate well with the divergence of the innovations process computed by EKF-1, as shown in Fig. 7 for the three measurement components, ψ, θ, and r. The last result bears a special significance because the implementation of the SPRT in this case is based on the innovations process as computed by the two filters.

3. Search Radar

In this case the launch location and the launch azimuth angle are unknown, as in the earlier case. The time from launch until target acquisition t_0 is assumed to be uniformly distributed over the interval [0, 3] s. The statistical moments of the initial state vector are summarized in Tables 2 and 3. The process noise intensity used in this case is $Q_{\text{st}}(t) = 0$.

Figure 8 shows the estimation performance of EKF-0 in a typical case, where the missile launched is SCUD-C. In this particular example, the TBM was launched 3 s before acquisition, while the estimator assumed initially that $t_0 = 0$ s. Excellent estimation performance is demonstrated for all estimated state variables, including the launch time. On the other hand, Fig. 9 shows the performance of EKF-1 in the same case. Because this filter's model (assuming SCUD-B) does not match the true system's state (corresponding to SCUD-C), this filter diverges in almost all state variables, as could be expected.

B. Monte Carlo Simulation Results

To statistically assess the performance of the method, a 600-run Monte Carlo simulation study (300 runs for each TBM) was conducted in both the staring radar and the search radar cases. In each of these cases, the associated unknown TBM launch parameters (launch location, azimuth angle and time) were randomly sampled from their assumed respective distributions.

Table 2 Mean of initial state vector

$\mu(0)$ component	Staring radar	Search radar
$\mu_x(0)$, m	0	0
$\mu_y(0)$, m	0	0
$\mu_z(0)$, m	0	0
$\mu_v(0)$, m/s	0	0
$\mu_\chi(0)$, deg	0	0
$\mu_\gamma(0)$, deg	90	——
$\mu_{t_0}(0)$, s	——	1.5

Table 3 Covariance of initial state vector

diag$\{P(0)\}$ entry	Staring radar	Search radar
$P_x(0)$, m^2	10^6	10^6
$P_y(0)$, m^2	10^6	10^6
$P_z(0)$, m^2	10^4	10^4
$P_v(0)$, m^2/s^2	0	0
$P_\chi(0)$, deg^2	0	100
$P_\gamma(0)$, deg^2	100	——
$P_{t_0}(0)$, s^2	——	0.75

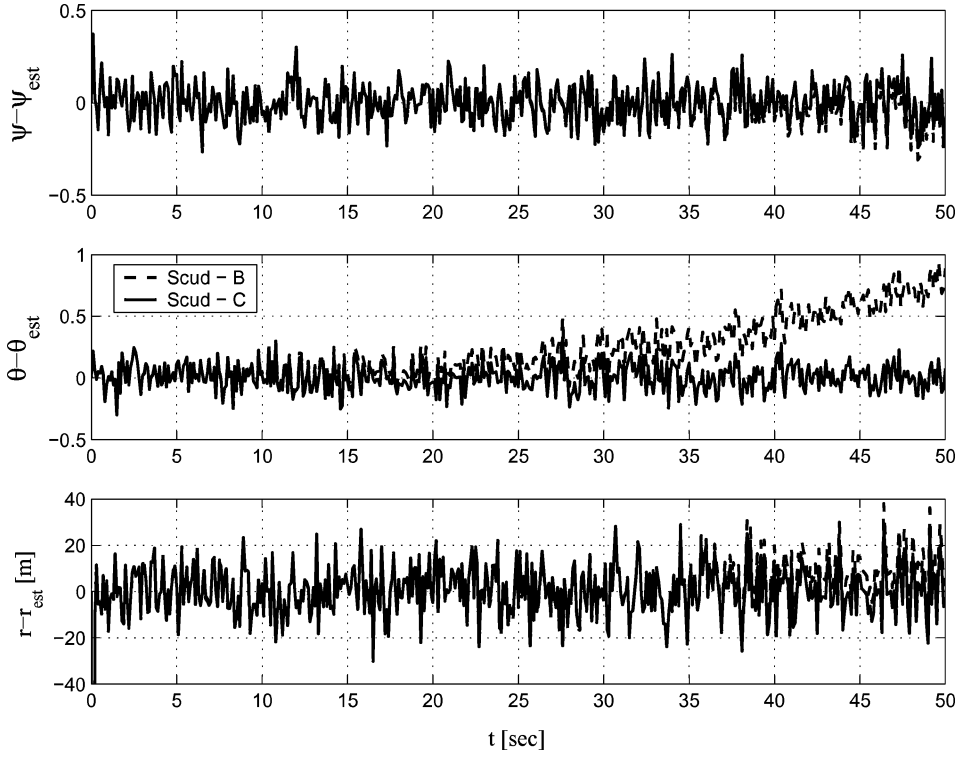

Fig. 7 EKF-0 (assuming SCUD-C launch) and EKF-1 (assuming SCUD-B launch) innovations process in a case of a SCUD-C launch; staring radar.

1. Nominal Performance

The first phase of the simulation assumed nominal parameters for the TBM's mathematical model (i.e., no parameter uncertainty). The resulting mean identification times and the observed error rates are shown in Table 4. In both cases, the observed error rates differ from their corresponding predetermined values. This can be explained by noting that the SPRT is driven by the innovations process as computed by the EKF; thus, the identification time and the error

Table 4 Monte Carlo simulation study results with nominal parameters

Observed performance	Staring radar	Search radar
SCUD-C mean identification time (s)	13.2	14.7
SCUD-B mean identification time (s)	15.6	15
Observed false-alarm rate	0	0.0033
Observed missed-detection rate	0.017	0.01

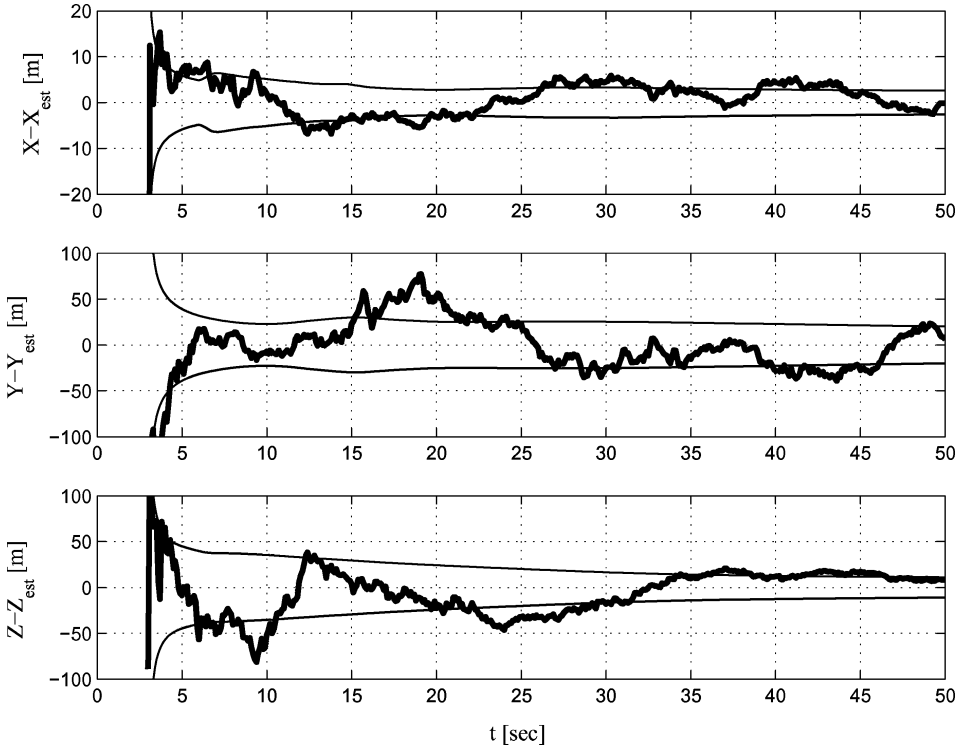

a) x, y, z

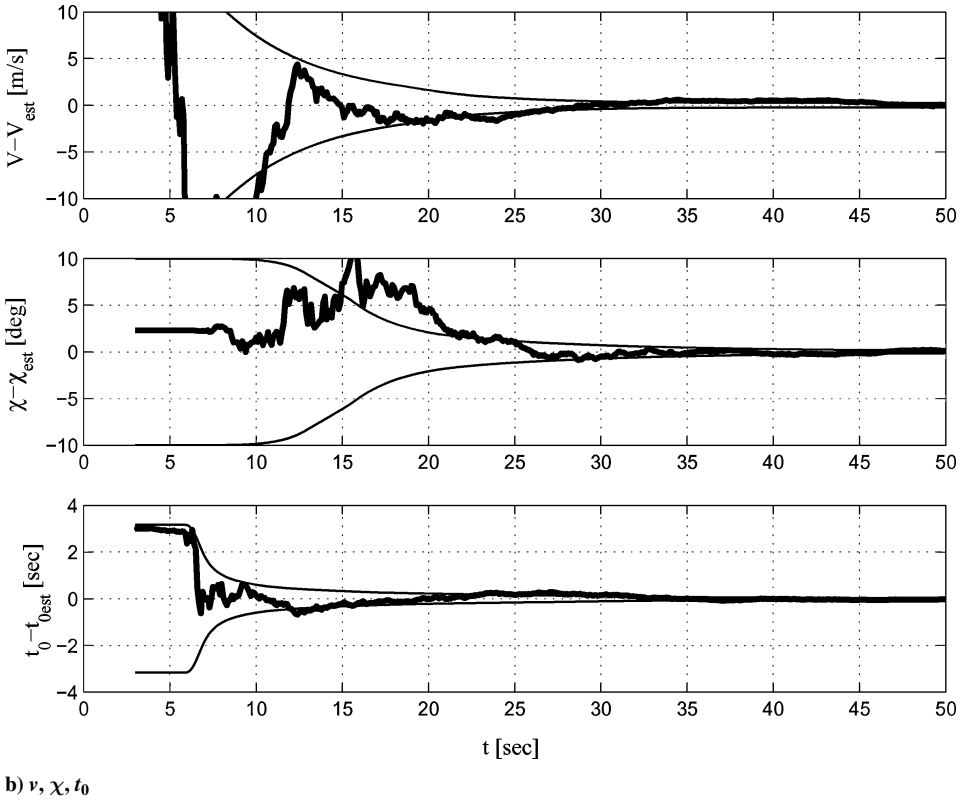

b) v, χ, t_0

Fig. 8 EKF-0 estimation performance for a SCUD-C launch; search radar: ——, estimation error; ——, 1-σ envelope (as computed by the filter).

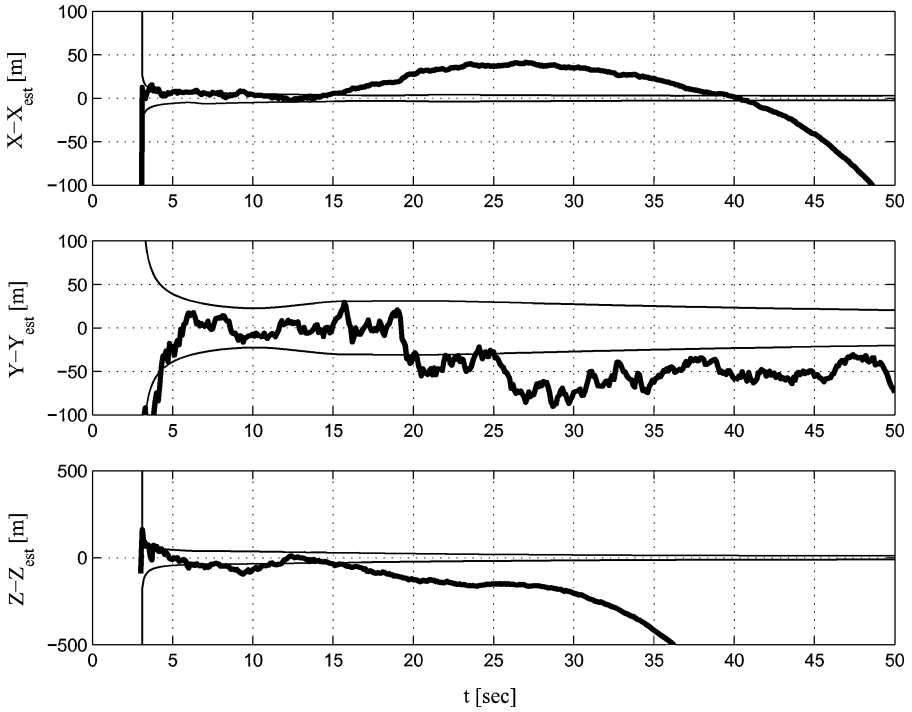

a) x, y, z

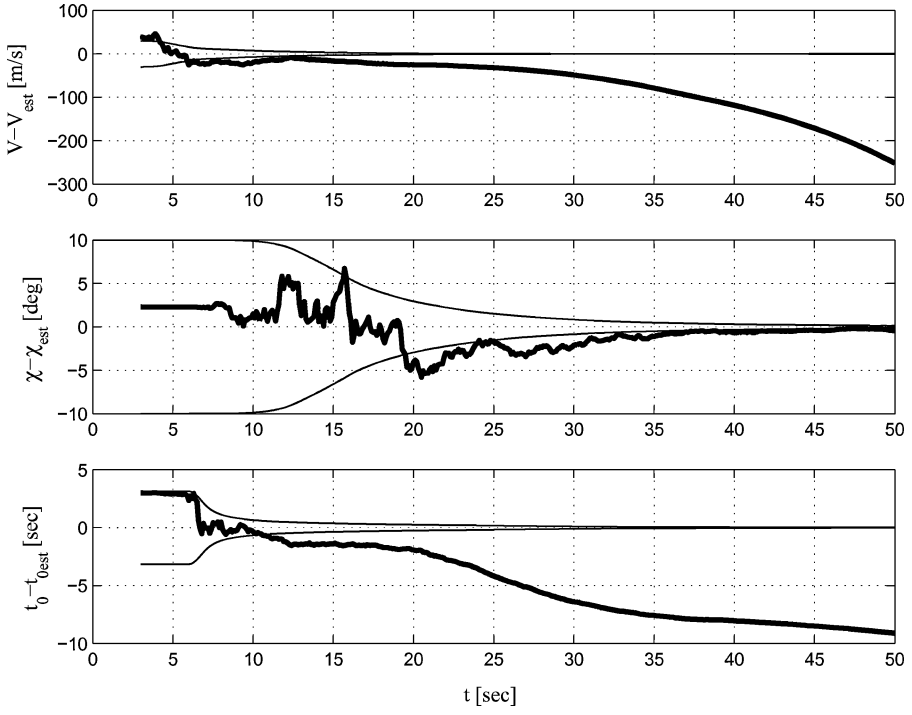

b) v, χ, t_0

Fig. 9 EKF-1 estimation performance for a SCUD-C launch; search radar: ——, estimation error; ——, 1-σ envelope (as computed by the filter).

rates depend, to some extent, on proper filter tuning. Also, as could be expected, the identification times have almost doubled relative to the complete information case. The identification times for the search radar case, where the launch time is unknown, are not significantly different than those for the staring radar case, where the launch time is assumed known. This can be attributed to the high accuracy of the state estimators used and, in particular, to the accurate estimation of the launch time.

2. Performance in the Presence of Parameter Uncertainty

In the second phase of the Monte Carlo simulation, some uncertainty was assumed in the TBM's mathematical model main parameters. This case was run to analyze the sensitivity of the proposed identification algorithms to variations in the underlying mathematical model. When missile parameter uncertainties are considered, the identification problem becomes more difficult because the feasible missile trajectory envelopes become very similar. Thus, it becomes more difficult to statistically distinguish between the missiles, and it can be expected that the mean identification times will be longer (because more measurements are required to reach a statistically significant decision in the presence of uncertainty).

Variations in the following parameters were assumed: initial mass, mass reduction rate, drag coefficient, and TBM acceleration command. Monte Carlo simulation runs were performed where these

Table 5 3-σ variations in TBM model parameters

Parameter	Variation, %
m_0, kg	4
$\dot{m}$, kg/s	4
c_d	15
a_n^C, m/s^2	15

Table 6 Process noise intensity matrix diagonal entries (uncertain parameters)

Intensity entry	Staring radar	Search radar
q_x, m^2/s	0	4000
q_y, m^2/s	0	490
q_z, m^2/s	0	90
q_v, m^2/s^3	8.1	0.9
q_χ, deg^2/s	10^{-3}	0
q_γ, deg^2/s	0	——
q_{t_0}, s	——	0

Table 7 Monte Carlo simulation study results with parameter uncertainty

Observed performance	Staring radar	Search radar
SCUD-C mean identification time (s)	21.8	21.5
SCUD-B mean identification time (s)	18.7	20.5
Observed false-alarm rate	0.027	0.04
Observed missed-detection rate	0.033	0.02

parameters were sampled from uniform distributions over intervals centered about the nominal parameter values. The 3-σ values of these distributions are summarized in Table 5.

To enable the EKF to deal with parameter uncertainties, its bandwidth was increased. This was done by using the process noise intensity matrix given in Table 6.

Monte Carlo simulations of 300 launches for each TBM resulted in the mean identification times and observed false-alarm and missed-detection rates as shown in Table 7. As could be expected, the mean identification times in the presence of parameter uncertainty are longer, and the error rates are increased relative to the nominal case. Nevertheless, the overall performance of the method is still acceptable in both staring and search radar cases, with relatively small error rates (albeit larger than the predetermined thresholds) even in the presence of modeling errors.

V. Conclusions

The problem of deciding between two theater ballistic missiles in an uncertain environment using a minimal number of radar measurements was addressed. Decision algorithms based on Wald's SPRT were developed for several scenarios of increasing complexity. When the missiles' models, as well as their launch location and time, are completely known, the SPRT works directly with the raw measurements. In more practical scenarios, when some of the launch parameters are unknown, the identification algorithms use the innovations processes, computed by extended Kalman filters, to drive the SPRT. A Monte Carlo simulation study was used to demonstrate the performance of the proposed algorithms. When the launch parameters are completely known, the observed false-alarm and missed-detection rates are identical to the prespecified probability values. In more practical cases, where the launch parameters are partially or completely unknown, the identification times and the observed error rates depend on proper filter tuning, as could be expected. Nevertheless, the simulation study demonstrates the method's viability and robustness, with mean identification times of about 20 s, corresponding to error rates of a few percent, even in the presence of considerable missile parameter uncertainty.

As a final note, it should be emphasized that although this paper has addressed the problem of distinguishing between just two theatre ballistic missiles, more complex problems, involving more than two missiles, can be handled similarly using extensions of the methods presented herein. Such extensions can be based on M-ary SPRT techniques that have been introduced in the literature.

Acknowledgment

This work is based on the first author's Master's thesis in the Department of Aerospace Engineering at the Technion—Israel Institute of Technology.

References

[1]Philips, H. E., "PAC-3 Missile Seeker Succeed," *Aviation Week and Space Technology*, Vol. 150, No. 12, 1999, p. 30.

[2]Hughes, D., "Next Arrow Test This Summer After Scoring Direct Hit," *Aviation Week and Space Technology*, Vol. 146, No. 12, 1997, p. 34.

[3]Shima, T., Oshman, Y., and Shinar, J., "Efficient Multiple Model Adaptive Estimation in Ballistic Missile Interception Scenarios," *Journal of Guidance, Control, and Dynamics*, Vol. 25, No. 4, 2002, pp. 667–675.

[4]Guelman, M., "Boost Phase Interception of Ballistic Missiles," in *Ballistic Missiles: The Threat and The Response*, edited by A. Stav, Ariel Center for Policy Research (ACPR) Publishers and Brassey's Ltd., Shaarei Tikva, Israel and London, 1999, pp. 241–249.

[5]Wald, A., *Sequential Analysis*, Wiley, New York, 1947, Chaps. 2 and 3.

[6]Bhanu, B., "Automatic Target Recognition: State of the Art Survey," *IEEE Transactions on Aerospace and Electronic Systems*, Vol. AES-22, No. 4, 1986, pp. 364–379.

[7]Roth, M. W., "Survey of Neural Network Technology for Automatic Target Recognition," *IEEE Transactions on Neural Networks*, Vol. 1, No. 1, 1990, pp. 28–43.

[8]Jouny, I., and Garber, F. D., "M-ary Sequential Hypothesis Test for Automatic Target Recognition," *IEEE Transactions on Aerospace and Electronic Systems*, Vol. 28, No. 2, 1992, pp. 473–483.

[9]Hancock, J. C., and Wintz, A. P., *Signal Detection Theory*, McGraw–Hill, New York, 1966, Chaps. 3 and 4.

[10]Deckert, J. C., Desai, M. N., Deyst, J. J., and Willsky, A. S., "F-8 DFBW Sensor Failure Identification Using Analytic Redundancy," *IEEE Transactions on Automatic Control*, Vol. AC-22, No. 5, 1977, pp. 795–803.

[11]Corsini, G., Dlle Mese, E., Marchetti, G., and Verrazzani, L., "Design of the SPRT for Radar Target Detection," *Proceedings of the IEEE*, Vol. 132, Part F, No. 3, 1985, pp. 139–148.

[12]Bussgang, J. J., "Sequential Methods in Radar Detection," *Proceedings of the IEEE*, Vol. 58, No. 5, 1970, pp. 731–743.

[13]Wald, A., and Wolfowitz, J., "Optimum Character of the Sequential Probability Ratio Test," *Annals of Mathematical Statistics*, Vol. 19, 1948, pp. 326–339.

[14]Shiryayev, A. N., *Optimal Stopping Rules*, Springer-Verlag, New York, 1977.

[15]Speyer, J. L., and White, J. E., "Shiryayev Sequential Probability Ratio Test for Redundancy Management," *Journal of Guidance, Control, and Dynamics*, Vol. 7, No. 5, 1984, pp. 588–595.

[16]Mendel, J. M., *Lessons in Digital Estimation Theory*, Prentice–Hall, Englewood Cliffs, NJ, 1987, p. 150.

[17]Duncan, L. (ed.), "Strategic Weapon Systems," No. 34, Janes' Information Group Ltd., Sentinel House, Surrey, England, UK, 2001, pp. 110–113.